Probing the Ordering of Semiconducting Fluorene−Thiophene Copolymer Surfaces on Rubbed Polyimide Substrates by Near-Edge X-ray Absorption Fine Structure

Lisa R. Pattison,*,† Alexander Hexemer,† Edward J. Kramer,*,†,‡ Sitaraman Krishnan,# Pierre M. Petroff,†,§ and Daniel A. Fischer⊥

Department of Materials, University of California Santa Barbara, Santa Barbara, California 93106; Department of Chemical Engineering, University of California Santa Barbara, Santa Barbara, California 93106; Department of Electrical Engineering, University of California Santa Barbara, Santa Barbara, California 93106; National Institute of Standards and Technology, 100 Bureau Drive, Stop-8523, Gaithersburg, Maryland 20899; and Department of Materials Science and Engineering, Bard Hall, Cornell University, Ithaca, New York 14853

Received October 10, 2005; Revised Manuscript Received January 12, 2006

ABSTRACT: The temperature-dependent alignment of semiconducting liquid crystalline fluorene−thiophene copolymer (F8T2) thin film surfaces was investigated using the near-edge X-ray absorption fine structure (NEXAFS) technique. Partial electron yield spectra were recorded over a range of temperatures in order to observe directly the surface orientation as the polymer is heated and cooled through glass, crystal, and liquid crystal phases. In addition, samples annealed under varying processing conditions and quenched to room temperature were analyzed. The NEXAFS data show that (a) in thin F8T2 films at all temperatures the polymer backbone lies in the plane of the substrate, (b) the fluorene and thiophene rings are rotated randomly about the molecular axis, (c) orientation of the polymer backbone can be controlled using a rubbed polyimide alignment layer as a template for liquid crystal orientation, and (d) under proper annealing conditions there is strong temperature-dependent alignment of the copolymer main-chain axis to the rubbing direction which extends from the polyimide/F8T2 interface all the way to the F8T2 surface. The surface alignment does not disappear after annealing at temperatures ∼30 K above the bulk nematic to isotropic transition.

Introduction

Conjugated organic polymers are increasingly being developed as functional materials for various devices including organic thin film transistors (OTFTs), photovoltaics, and organic light-emitting diodes (OLEDs). The importance of alignment of the stiff conjugated main chain for enhancing specific electronic properties of these devices is widely recognized.[1−7] Higher carrier mobilities and polarized photon emission are usually obtained when the conjugated polymer films are macroscopically ordered. For this reason polyfluorenes and other self-aligning, liquid crystalline conjugated polymer semiconductors have attracted much recent attention.

Poly(9,9-dioctylfluorene-*co*-bithiophene) alternating copolymer (F8T2) has several characteristics that make it convenient for studying electrical characteristics of aligned polymer films: conjugated segments for charge transport, relatively good stability in air, and solubility in a wide range of solvents. It also exhibits a thermotropic liquid crystal phase since F8T2 is a main-chain liquid crystal polymer of the "hairy rod" type (see Figure 1 and Figure 2 inset). The octyl side chains protruding from the rodlike backbone (hence the name "hairy rod") facilitate solvation in organic solvents.

Previous studies have shown how the liquid crystal phase of polyfluorene materials can be advantageous in achieving main-chain alignment.[6,8−11] Polarized UV−vis spectroscopy and polarized light microscopy showed that F8T2 thin films deposited on rubbed polyimide alignment layers can be macroscopically aligned when annealed in the nematic phase. The polymer chain alignment and charge carrier mobility for the F8T2 molecules presented in this study are strongly correlated. We found that when polymer chains were aligned parallel to the transistor channel length, the field-effect mobility values

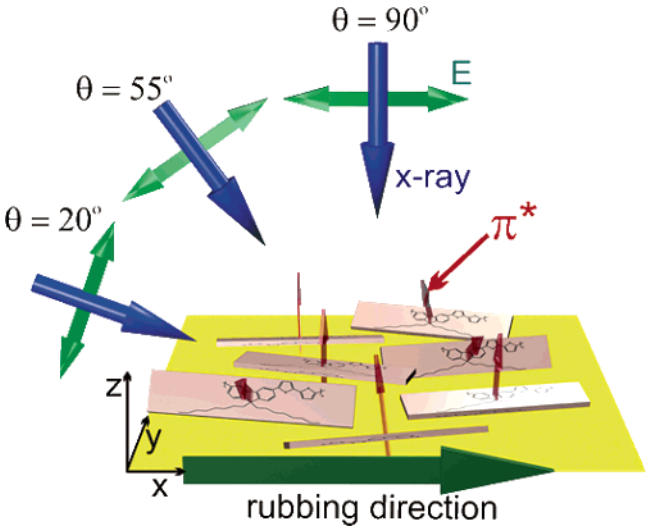

Figure 1. NEXAFS geometry for the parallel configuration in which the sample is rotated about the *y*-axis with respect to the electric field vector (**E**). At normal incidence ($\theta = 90°$), **E** is parallel to the rubbing direction, **x**. Red arrows represent the C 1s to π^* transition dipole moments of the F8T2 molecules, and for a nematic aligned perfectly along the rubbing direction these vectors would all be normal to **E** at $\theta = 90°$. For the perpendicular configuration, the F8T2 sample is rotated by 90° about the *z*-axis.

† Department of Materials, UCSB.
‡ Department of Chemical Engineering, UCSB.
§ Department of Electrical Engineering, UCSB.
⊥ National Institute of Standards and Technology.
Cornell University.
* To whom correspondence should be addressed. E-mail: lkinder@engineering.ucsb.edu; edkramer@mrl.ucsb.edu.

10.1021/ma0521912 CCC: $33.50
Published on Web 02/22/2006

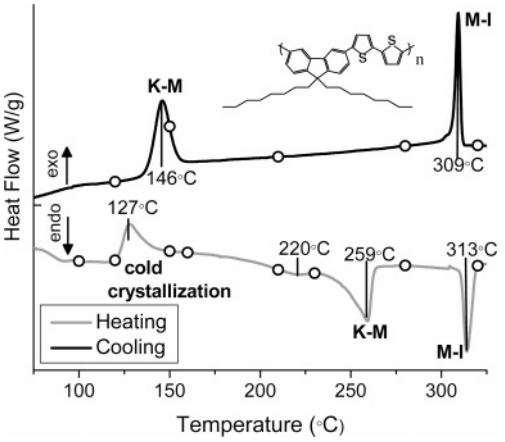

Figure 2. DSC thermogram for F8T2 in heating (gray) and cooling (black) at a rate of 10 °C/min. K = solid phase, M = mesophase, I = isotropic. Open circles indicate the temperatures at which NEXAFS spectra were taken. Inset shows the chemical structure of F8T2.

are 2−3 times greater than mobility for as-deposited (amorphous) films and 4−6 times greater than values obtained for devices with channel lengths perpendicular to polymer chain alignment.[10]

Evidence of bulk polymer alignment on rubbed polyimide alignment layers exists, yet we do not know whether this alignment persists throughout the film to the surface. For certain device architectures in OTFTs, photovoltaics, and OLEDs, the alignment of the top surface will play a large role in the device performance. For instance, in OLEDs and photovoltaics, the F8T2 alignment affects charge injection and separation at the interfaces, and for noninverted transistor structures, the top surface of the semiconductor is crucial to the carrier mobility, since this is the region of current flow in the transistor operation.

To obtain information on the molecular orientation at the polymer surface, carbon K-edge soft X-ray absorption spectroscopy, in particular the analysis of the near edge X-ray absorption fine structure (NEXAFS) and its polarization dependence, is used. When the soft X-ray radiation is polarized in the direction of the transition dipole moment of the electron orbitals of the molecule, it can be absorbed. The absorption results in the excitation of an electron from the core shell to an excited state. When the core hole fills, either an X-ray photon (fluorescence) or an Auger electron is emitted. Emitted Auger electrons come dominantly from the top 2 nm of the thin film[12] and are detected by an electron channeltron detector. In the case of π-bonding (conjugated molecules), the transition dipole moment of the π^* orbital is oriented perpendicular to the C=C bond direction and, therefore, perpendicular to the molecular axis. Thus, the absorption probability for polarized X-rays depends on the relative orientation of the molecular axis and the electric field vector of the incident X-rays. The dependence of the C 1s to π^* resonance on the polarization of the electric field of the incident X-rays thus gives information about the preferential orientation of the conjugated polymer backbone. From the polarization dependence, order parameters can be derived, and a quantitative description of the molecular orientation can be achieved. Thus, using NEXAFS, we have a direct measure of the amount of X-rays absorbed, and correspondingly, the degree of alignment of the surface molecule to the polarization of the X-ray beam.

Recently, Jung et al. investigated the surfaces and bulk alignment of polyfluorene polymers using the NEXAFS technique.[13] However, rather than using polyimide alignment layers, buffing of the polyfluorene thin film surface was used to achieve preferential reorientation of the polyfluorene molecular axis along the rubbing direction at the surface. This reorientation occurred at the thin film surface, as evidenced by Auger electron yield, but was greatly reduced in the bulk, according to total electron yield measurements. In addition, upon heating a rubbed polyfluorene film in its nematic melt state (170 °C), the rubbing-induced reorientation of polymer molecules completely disappears.

In this work, we look at the reorientation of fluorene−thiophene copolymer induced by deposition on a rubbed polyimide alignment layer after various thermal treatments. We use NEXAFS to determine the molecular orientation at the surface, observing the strong alignment of the F8T2 main-chain axis to the rubbing direction and the temperature stability of these results. Moreover, we observe the effects of various annealing conditions on the NEXAFS spectra and also take NEXAFS data *during* annealing in a vacuum. Together with the previously published X-ray diffraction data and polarization data, the present results indicate ordering throughout the polymer thin film.

Experimental Methods

The F8T2 material used in these experiments was supplied by Dow Chemical. From gel permeation chromatography, using tetrahydrofuran as eluting solvent and polystyrene standards, the compound has a M_w of 31.3 kg/mol, M_n of 14.1 kg/mol, and a PDI of 2.1. Heavily doped n+ silicon wafers were used as the substrates in order to avoid sample charging. These wafers were prepared for F8T2 deposition by spin-coating with Nissan Chemical polyimide RN1340. The polyimide precursor is spin-cast onto a clean Si wafer, heated in atmosphere on a hot plate for 10 min at 85 °C, and then baked in an oven at 285 °C for 90 min to form a polyimide film. The polyimide is then rubbed using a Yoshikawa Chemical Co. YA-20-R cloth. Rubbing the polyimide aligns the surface molecules along the rubbing direction, creating an asymmetry in the molecular bonds at the surface. The unidirectional molecular alignment at the surface of the rubbed polyimide provides a template for the F8T2 orientation when heated to the mesophase.[14−18] The F8T2 polymer films were spin-coated onto prepared substrates from 1% (10 mg/mL) solutions in xylenes. Scanning force microscopy shows that the film thickness is ∼90 nm, which is around the target thickness for active layers in organic electronic devices.

Partial electron yield NEXAFS spectra were acquired at the NIST/Dow materials characterization end station on the U7A beamline at the National Synchrotron Light Source at Brookhaven National Laboratory. The beamline is equipped with a toroidal mirror spherical grating monochromator that gives this beamline an incident photon energy resolution and intensity of 0.2 eV and 5×10^{10} photons/s, respectively, for an incident photon energy of 300 eV and a typical storage ring current of 500 mA. The X-ray beam is elliptically polarized, with the electric field vector dominantly in the plane of the storage ring (polarization factor = 0.85). The end station is equipped with a heating/cooling stage positioned on a goniometer that controls the orientation of the sample with respect to the polarization vector of X-rays. The partial electron yield (PEY) is collected using a channeltron electron multiplier with an adjustable entrance grid bias. All the data reported here are for a grid bias of −150 V. The spot diameter of the X-ray beam on the sample at normal incidence is ∼0.1 mm. Energy calibration was done using a highly oriented pyrolytic graphite (HOPG) reference sample. The HOPG 1s to π^* transition was measured on the U7A beamline and assigned a peak value of 285.5 eV according to the literature value.[19] The simultaneous measurement of a graphite-coated gold grid allows then the calibration of the photon energy with respect to the HOPG sample.

The carbon K-edge NEXAFS spectra were recorded at angles θ = 90°, 80°, 70°, 60°, 55°, 40°, 30°, and 20°, where θ is the angle between the electric field vector (**E**) of the polarized soft X-rays and the sample normal as well as the angle between the incident photon beam and the sample surface (Figure 1). The samples were

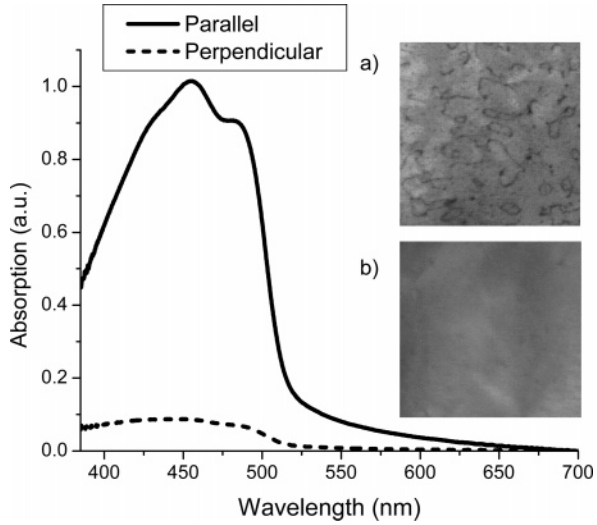

Figure 3. F8T2 thin film absorption of UV−vis light polarized parallel (solid line) and perpendicular (dashed line) to the rubbing direction. Experiment performed after quenching F8T2 from the mesophase. Inset: optical micrograph (250 μm × 250 μm) of film under crossed polarizers (a) upon reaching 280 °C and (b) after 10 min anneal at 280 °C.

on rubbed polyimide alignment layers and thus were tested in parallel and perpendicular geometry. The parallel geometry, in which **E** at $\theta = 90°$ is parallel to the rubbing direction, **x**, is depicted in Figure 1. For the perpendicular experimental configuration, the F8T2 sample is rotated about the *z*-axis 90° such that the **E** vector at $\theta = 90°$ is perpendicular to the rubbing direction, parallel to **y**.

Results and Discussion

Structure of the Bulk. Using differential scanning calorimetry (DSC), we identify the phase transition temperatures at which F8T2 becomes liquid crystalline and isotropic in the bulk. Figure 2 shows DSC curves of F8T2 in the first heating and cooling cycles at scanning rates of 10 °C/min in N_2. Phase changes are accompanied by a release or intake of thermal energy, represented respectively by peaks or dips in the DSC scan. On heating, there is an exotherm at 127 °C representing cold crystallization. At 220 and 259 °C there are endotherms in the thermogram indicating transitions from the crystalline solid (K) phase to the nematic liquid crystal mesophase (M). A sharp endotherm corresponding to the nematic to isotropic transition occurs at 313 °C. The occurrence of two peaks during the K−M transition could indicate the complexity of melting in a polymer chain material with a high polydispersity index.

As deposited from xylene solutions, F8T2 films are amorphous. Annealing at temperatures within the liquid crystal range creates ordered domains, but such films lack long-range orientational order since individual domains are not all oriented in a specific direction. However, when F8T2 is deposited on rubbed polyimide surfaces, well-ordered, monodomain films can be made.[8,9] F8T2 molecules close to the interface lie with their long axes along the rubbing direction. Neighboring molecules align with these underlying molecules when heated to the mesophase. Figure 3 shows a thin F8T2 film ∼100 nm thick on a glass substrate coated with a 40 nm thick rubbed polyimide (PI) alignment layer. When this sample is annealed at 280 °C under N_2, liquid crystal domains and threadlike disclination defects characteristic of nematic order appear in polarized light microscopy (PLM) images (Figure 3a). Holding this temperature for 10 min anneals out the defects, leaving a monodomain at least as large as the image area (250 × 250 μm) and much larger than the active area of a device (Figure 3b).

To estimate the degree of orientation achieved, the quenched sample was analyzed with polarized UV−vis absorption spectroscopy (Figure 3). Light polarized parallel to the polyimide rubbing direction was strongly absorbed, whereas perpendicularly polarized light showed only weak absorption. Hence, the UV−vis transition dipole moment of the chromophores is oriented predominantly in the rubbing direction. Using the dichroic ratio at the absorption maximum, a macroscopic order parameter can be calculated $S \geq (A_{||} - A_{\perp})/(A_{||} + 2A_{\perp}) = 0.78$, indicative of a high degree of alignment.

The observation of uniform birefringence in PLM indicates homogeneous alignment of the F8T2 main-chain axes lying in the plane of the substrate rather than perpendicular to the surfaces as is seen in homeotropic alignment. More importantly, we can infer from X-ray diffraction studies that polyfluorenes and fluorene−thiophene copolymers in the crystalline phase lie with their backbone in the plane of the substrate and that the spacing between these chains is governed by the length of alkyl side chains.[9,10,20] For our macromolecule with octyl side chains, X-ray diffraction showed a stacking distance parallel to the film normal of 16 Å.[10]

Structure of the F8T2 Surface. In Figure 4a,b we show the C K-edge NEXAFS partial electron yield (PEY) signal as a function of soft X-ray photon energy. Peaks in the PEY spectra arise at energies required to excite a 1s core electron to an unoccupied molecular orbital. An unambiguous peak assignment for all spectral features is difficult and not critical for the purpose of this work. These data were taken from a sample annealed at 280 °C and measured at room temperature, but the peak positions do not change with temperature, nor do new peaks appear (for example, from oxidation/degradation of the films during heating and probing). The peak with strongest intensity at 285.2 eV is the result of the transitions of electrons from the C 1s to π^* orbitals of the conjugated C═C segments in both the fluorene and thiophene rings.[13] The transition dipole moment (TDM) of π^* orbitals is normal to the plane of conjugation and thus normal to the main chain (molecular) axis of the conjugated chain. The absorption structure at 287.6 eV is the result of 1s to σ^* transitions due to C−S and C−H bonds. The broad structure centered around 293.2 eV is due to 1s to $\sigma^*$of C−C bonds. Our discussion will focus on the intensity variations of the first resonance at 285.2 eV, which indicates the changes in concentration and orientation of the π^* TDMs. The π-conjugated bonds are responsible for the electronic and optoelectronic effects necessary for device applications and are of most interest for our study.

In this work, we present two types of temperature-dependent data. First, we show postanneal scans of the samples. In this case, F8T2 films on rubbed polyimide are subjected to the thermal annealing procedure prior to entering the NEXAFS sample chamber where they are measured at room temperature. Each sample underwent one temperature process including a brief (5, 10, or 20 min) anneal at a target temperature followed by rapid cooling to room temperature to enable freezing of the polymer in the structure it had in the high-temperature phase. All thermal treatment of the F8T2 films was performed under vacuum. Target temperatures were chosen at significant points along the DSC curve in order to characterize different phases and transitions. The temperatures studied are indicated by open circles on the DSC curve in Figure 2. Thermal processing was tailored such that we had samples corresponding to both the heating and cooling DSC curves. Samples representing the heating curve were heated only to the target temperature where they were annealed before cooling to room temperature. For

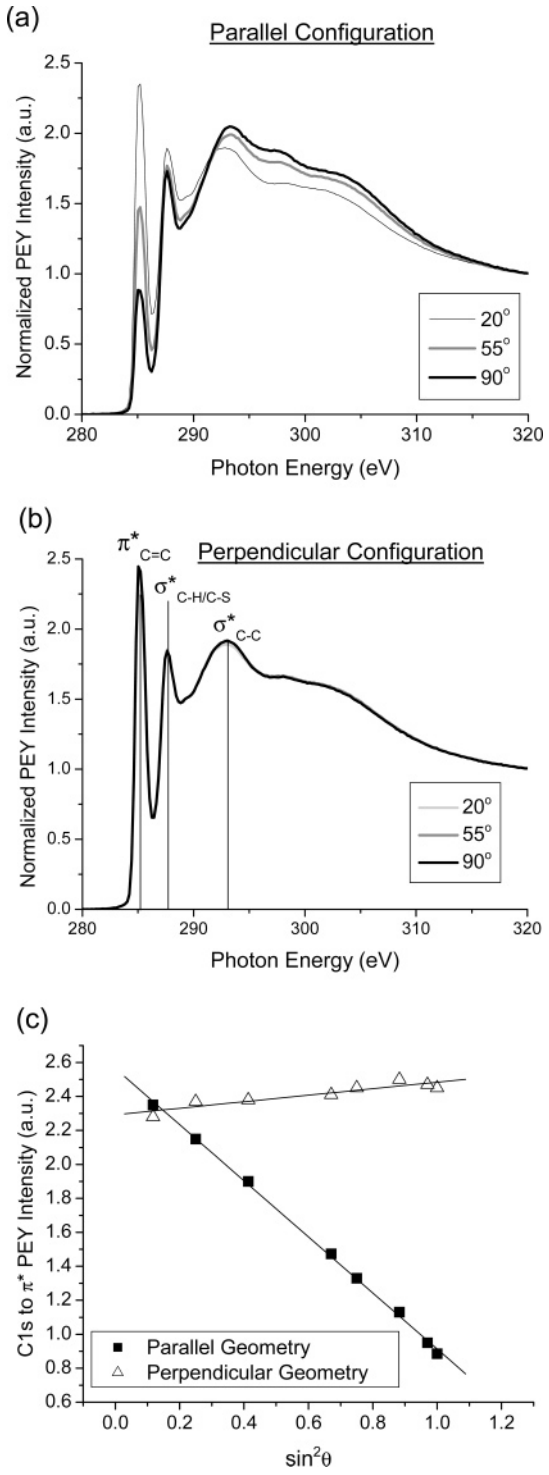

Figure 4. PEY data for F8T2 postanneal thin film sample that was annealed at a temperature of 280 °C and then quenched to room temperature. Scans taken at room temperature at $\theta = 20°$, 55°, and 90° incidence in the parallel (a) and perpendicular (b) geometries. The strong overlap of curves in (b) makes it difficult to distinguish between the three scans. (c) shows the peak intensity of the C 1s to π^* transition plotted against $\sin^2\theta$ with a linear fit whose slope and intercept parameters were used in the calculation of S and η as described in the text (see text).

the cooling curve, spin-cast F8T2 films were heated to above the nematic−isotropic (M−I) transition (313 °C), cooled to the target temperature where they were annealed, and then rapidly brought to room temperature. Three different annealing times were probed so that we could investigate the phase transformation kinetics. We found that there was no significant difference in samples annealed for only 5 min and samples annealed for 20 min. Hence, all data presented here will be from samples annealed for 20 min.

In addition to the postanneal scans, we also made in-situ NEXAFS measurements on F8T2 films at different temperatures. In this case, we put two large area F8T2 films (one in the parallel and one in the perpendicular configuration) spin-cast on rubbed polyimide onto a sample stage with a heating element. The samples were heated from room temperature to the first point along the DSC curve at 150 °C, held for 10 min, and then measured using NEXAFS. All the points along the heating and cooling curve were taken this way on the same two samples under vacuum. Though the same samples were used for all of the in-situ temperature measurements, the beam was moved to a different spot on the sample for successive scans to prevent radiation damage. We also tested for radiation damage on a test sample by heating to 150 °C, measuring the sample, irradiating with the soft X-ray beam at $E = 150$ eV for 5 h, and measuring again. The PEY spectra did not change, so we believe that radiation effects for these samples are minimal. For these in-situ measurements, temperature was controlled to within ±5 °C during measurement, and the temperature was stable for 10 min before the scan was started.

Figure 4a shows the postanneal polarization dependence of the PEY NEXAFS signal for a parallel configuration sample heated to 280 °C and rapidly cooled to room temperature. Shown in the figure are the NEXAFS PEY intensities at $\theta = 90°$, 55°, and 20° X-ray incident angles. The PEY spectra that were measured at intermediate angles (30°, 40°, 60°, 70°, and 80°) lie between the 90° and 20° extremes but are left out of plots for clarity. As shown in Figure 4a, the NEXAFS PEY intensity at 20°, 55°, and 90° differs for the C=C 1s to π^* resonance at 285.2 eV. At 90° the rubbing direction is parallel to the electric field vector of the incident soft X-ray radiation (parallel configuration). In this case, absorption is low because the electric field vector lies along the main-chain axis, whereas the TDM of π^* orbitals are perpendicular to this axis. As expected, there is stronger absorption at a 20° angle of incidence, where a large component of the electric field vector of incident radiation is out of plane, and the NEXAFS signal decreases with increasing angle.

In the case of perpendicular geometry, the angular dependence provides information as to the orientation of the aromatic rings about molecular chain axis, i.e., whether the rings are in the plane of the substrate, normal to the surface, or rotated at random. In the perpendicular configuration, the sample is being rotated about the main-chain axis with respect to the electric field vector of the incident soft X-ray radiation. Absorption occurs when the TDMs of the π^* orbitals are parallel to the electric field vector of the incident X-rays. In Figure 4b, we see that the 20°, 55°, and 90° 1s to π^* resonances overlap. This indicates that the orientation of the aromatic rings at the surface is nearly random. Because the π-conjugation along the backbone of F8T2 results in a rigid-rod molecule, we believe that each F8T2 polymer molecule is a rigid, planar unit, but neighboring molecules possess different rotational orientation,[21] as depicted in the sketch in Figure 1.

By comparing the intensity of the PEY signal in the perpendicular and parallel configurations, an assay of how well the main chain is aligned to the buffing direction of the polyimide can be obtained. We analyze the data using the method of Stöhr and co-workers[15,22] to provide a quantitative description of the ordering. Analysis showing the dichroic ratio is presented elsewhere.[11] For our macromolecular system, we

assume that the surface tilt angle,[15] γ, is equal to zero. We use three TDM orientation factors (f) to describe the relative alignment of the transition dipole moment of the π^*-orbital along three orthogonal axes: x (rubbing direction), y (in-plane perpendicular to rubbing direction), and z (surface normal).

$$f_x = \frac{A^{\perp} + B^{\parallel}}{I_{\text{tot}}} \tag{1a}$$

$$f_y = \frac{A^{\parallel} + B^{\perp}}{I_{\text{tot}}} \tag{1b}$$

$$f_z = \frac{A^{\perp} + B^{\parallel}\left(1 - \frac{1}{P}\right)}{I_{\text{tot}}} \tag{1c}$$

P is the polarization factor of the elliptically polarized X-ray beam (0.85), I_{tot} is the total integrated intensity, and A and B are coefficients from the linear equation describing the angular dependence of the intensity (I).

$$I(\theta) = A + B \sin^2 \theta \tag{2}$$

The normalization condition $f_x + f_y + f_z = 1$ yields the following expression for the total integrated intensity:

$$I_{\text{tot}} = \frac{3}{2}(A^{\parallel} + A^{\perp}) + \frac{3P - 1}{2P}(B^{\parallel} + B^{\perp}) \tag{3}$$

We have taken series of scans in the parallel configuration and in the perpendicular configuration. Since we have parallel and perpendicular cases, we define separately an $I^{\parallel}$, $I^{\perp}$, $A^{\parallel}$, $A^{\perp}$, $B^{\parallel}$, and $B^{\perp}$ by the following: $I^{\parallel}(\theta) = A^{\parallel} + B^{\parallel} \sin^2 \theta$ and $I^{\perp}(\theta) = A^{\perp} + B^{\perp} \sin^2 \theta$. Using the coefficients A and B, the values of the TDM orientation factors f_x, f_y, and f_z are obtained. f_x, f_y, and f_z (which are the projections of the TDM on the x, y, and z axes) can be used to find an order parameter (S) for the molecular axis and biaxiality (η) of the π^* orbitals about the rubbing direction.

A definition of the order parameter, S, of the molecular main-chain axis about the rubbing direction (**x**) can be obtained by considering the perpendicular relationship between the molecular axis and the C 1s to π^* TDM. When the molecular axis is oriented at an angle α from the x-axis, the TDM is oriented at an angle $(90° - \alpha)$ with respect to the x-axis. Since the orientation factor f_x represents the projection of the TDM onto the x-axis, $f_x = \cos^2(90° - \alpha) = 1 - \cos^2 \alpha$. Combining the value of f_x with the second Legendre polynomial expression for the structural order parameter, $S = {}^1/_2(3\langle\cos^2 \alpha\rangle - 1)$, we obtain an equation for the structural order parameter in terms of f_x:

$$S = \frac{1}{2}(2 - 3f_x) \tag{4}$$

The biaxiality defined in terms of f_y and f_z is

$$\eta = \frac{3}{2}(f_z - f_y) \tag{5}$$

S describes the average orientation of the molecular axes with respect to the x-axis (the rubbing direction).[23] The biaxiality, η, gives the preferential alignment of the π^* orbitals in the $y-z$ plane. Thus, $S = 0$, $\eta = 0$ describes the case where the molecular axes are randomly oriented along the three axes ($S = 0$), and the normals to the fluorene and thiophene units are oriented randomly about the molecular axes ($\eta = 0$). When S is positive, this is due to alignment of the molecular axes along the rubbing direction, **x** (TDMs of π^*-orbitals aligned in the $y-z$ plane directions), with $S = 1$ representing perfect alignment of the F8T2 main-chain axis along **x**. When S is negative, the main-chain axes are in the $y-z$ plane, and when all molecules lie in this plane, $S = -{}^1/_2$. When S is large and positive, $\eta < 0$ indicates a preference for the conjugated segments of the molecule to stand on edge ($f_y > f_z$), while $\eta > 0$ reflects a tendency for molecules to lie flat in the plane of the film ($f_y < f_z$).

Table 1. TDM Orientation Factors, Order Parameter, and Biaxiality for F8T2 in Heating (Bold) and Cooling (Italics)[a]

Temperature	f_x	f_y	f_z	S	η
Un-buffed 30°C	0.283	0.283	0.439	0.576	0.234
Un-buffed 120°C	0.278	0.278	0.445	0.583	0.251
Un-buffed 210°C	0.285	0.285	0.431	0.573	0.219
Un-buffed 280°C	0.284	0.284	0.433	0.574	0.224
Un-buffed 340°C	0.289	0.289	0.421	0.567	0.198
30°C	0.285	0.274	0.439	0.573	0.248
30°C	0.262	0.283	0.456	0.607	0.260
120°C	0.284	0.274	0.444	0.574	0.255
150°C	0.191	0.389	0.443	0.714	0.081
210°C	0.131	0.429	0.443	0.804	0.021
280°C	0.131	0.431	0.432	0.804	0.002
280°C	0.113	0.453	0.441	0.831	-0.018
340°C	0.208	0.396	0.391	0.688	-0.008
340°C	0.178	0.430	0.394	0.733	-0.054
280°C	0.141	0.440	0.415	0.789	-0.038
280°C	0.108	0.463	0.434	0.838	-0.044
210°C	0.113	0.462	0.417	0.831	-0.068
210°C	0.134	0.441	0.437	0.799	-0.006
150°C	0.087	0.458	0.452	0.870	-0.009
120°C	0.112	0.465	0.423	0.832	-0.063
30°C	0.078	0.481	0.441	0.883	-0.060

[a] To compare the postanneal scans (gray) with the in-situ temperature scans (white), the data are listed adjacently in the table. Data for unbuffed and buffed polyimide films are included as indicated.

Table 1 shows the data fitted using this analysis. We take the NEXAFS PEY spectra for angles ranging from 20° to 90° with the rubbing direction parallel and perpendicular to the polarization of the X-ray beam. We then plot the intensity vs $\sin^2 \theta$ to find A and B coefficients using a linear fit to eq 2 (see Figure 4c). Using A and B, we find the TDM orientation parameters f_x, f_y, and f_z, and with these, we calculate S and η. In Table 1, the molecular orientation factors, order parameter, and biaxiality are shown for postanneal and in-situ samples over a range of temperatures in heating and cooling. The first column shows the target temperature of the postanneal or in-situ heat treatment. Here, bold indicates the temperatures reached in heating, and italics represents cooling. Many temperatures are listed twice in a row because here we are comparing the postanneal data (highlighted in gray) to the in-situ data (white). Figure 5 shows plots of the calculated S and η values in heating and cooling for in-situ (a) and postanneal (b) data.

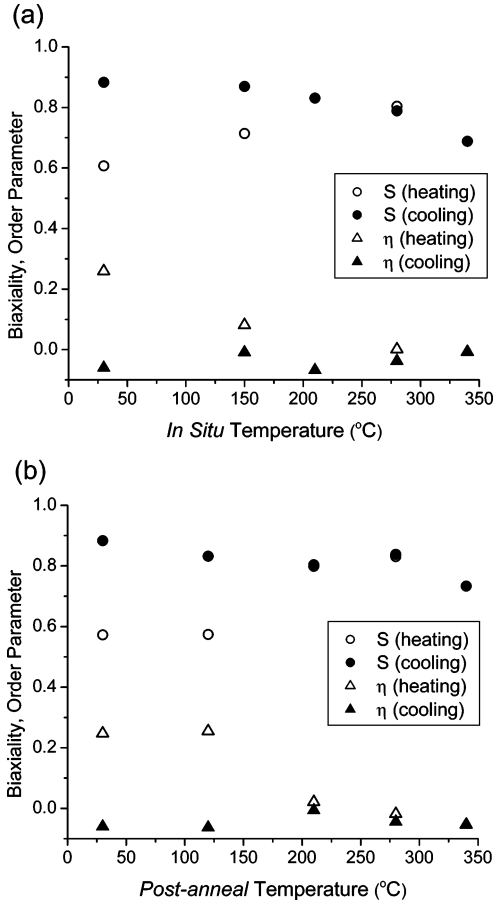

Figure 5. Nematic order parameter $0.5(2 - 3f_x)$ (circles) and biaxiality parameter $1.5(f_z - f_y)$ (triangles) vs annealing temperature for the samples analyzed in situ during annealing (a) and after annealing and quenching to room temperature (b). Open symbols, heating; closed symbols, cooling.

In addition to the data listed for buffed polyimide, data are also presented in Table 1 from samples that are deposited on unbuffed polyimide. Postanneal NEXAFS measurements taken after annealing these samples for 20 min at 120, 210, 280, and 340 °C are compared to an unannealed sample. The TDM orientation factors f_x and f_y are equal due to the lack of a buffing direction, and for all samples, values of $f_{x,y}$ lie in the range of 0.28−0.29. Values of f_z were in the range of 0.42−0.44. Using eqs 4 and 5, the orientational order parameter for these samples is around $S \sim 0.57$, and η ranges from 0.25 at low temperatures to 0.20 at 340 °C. Upon heating, the order parameter remains at ∼0.57 because the underlying polyimide has not been rubbed, and thus, there is no template for F8T2 alignment in the $x-y$ plane of the sample. The values of S are high even though the molecular axes are randomly oriented in the $x-y$ plane. This is a result of our definition of S, which assumes that all directions perpendicular to the director (**x**) are equivalent and therefore should not depend on the azimuthal angle. However, we know from X-ray diffraction and polarized light microscopy that the main-chain axes of long F8T2 molecules lie in the plane of the substrate (homogeneous alignment) rather than perpendicular to the surface as is seen in homeotropic alignment. For a perfectly homogeneous film, the lowest order occurs when the aromatic rings are randomly oriented about the molecular axes which are randomly oriented in the $x-y$ plane, $f_x = f_y = 0.25$ and $f_z = 0.5$. The corresponding values for S and η are 0.63 and 0.38, respectively. The values of $S \sim 0.57$ for samples on unbuffed polyimide are close to those expected for amorphous homeotropic films (with a small deviation probably due to some tilting of molecules in the z direction). Though the value of η is positive, this is not very meaningful unless there is alignment in the rubbing direction.[24]

Following the data for unbuffed samples in Table 1 are the data for buffed polyimide samples. As-deposited, the samples on buffed polyimide surfaces have the same values of S and η as the unbuffed polyimide samples because thermal treatment is required to align the molecules to the rubbing direction. All annealed samples show alignment along **x**, with S almost as large as 0.9 for samples that have been cooled through the nematic liquid crystal phase. For these aligned samples, $\eta \sim 0$, indicating that the normals to the fluorene and thiophene units are rotated randomly about the molecular axis, as illustrated in Figure 1.

We note that alignment of the molecular axis observed for the surfaces of our F8T2 films on rubbed polyimide alignment layers is considerably larger than that observed for polyfluorenes whose surface is rubbed after deposition.[13] From the values of the order parameter S_{TDM} and biaxiality (P) of the π^* TDM as defined by Jung et al. [$f_z = 0.33(2S_{TDM} + 1)$, $f_x = 0.33(1 - (S_{TDM} + P))$, $f_y = 0.33(1 - (S_{TDM} - P))$] and their values of $S_{TDM} = 0.23$ and $P = 0.21$ for the rubbed film, we find values of molecular order parameter and biaxiality of $S = 0.72$ and $\eta = 0.24$, respectively, using the definitions in eqs 4 and 5. In fact, the molecular alignment found after rubbing is comparable to the alignment we find at 340 °C above the nematic to isotropic transition. In addition, and quite apart from the possibility of damage to the polyfluorene from surface rubbing, our films are oriented through the film thickness.

Table 1 and Figure 5 show that when heated above 150 °C the structural order parameter is maximized ($S \sim 0.8$). This corresponds to the bulk DSC data (Figure 2), where the onset of the mesophase transition occurs at around 192 °C. A high degree of alignment persists throughout further annealing, until temperatures above the bulk nematic to isotropic transition temperature (340 °C) is reached. Even beyond the bulk nematic−isotropic transition temperature (313 °C), the large F8T2 molecule retains some orientation with the buffing direction, with $S \sim 0.7$. The most likely explanation for the persistence of the F8T2 alignment at temperatures above the bulk nematic−isotropic transition temperature is that the oriented polyimide layer exerts a surface field, stabilizing the nematic with reduced order. While it is possible that slow kinetics of reorientation might be responsible for retaining some nematic order, the fact that the oriented nematic forms within 5 min at 280 °C, well below the highest temperature of annealing where $S = \sim 0.7$ is retained even after 20 min equilibration time, suggests that this alternate explanation is unlikely.

The observation that the alignment of the molecular axes along the rubbing direction persists upon heating and cooling is an important conclusion because it provides an idea of the processing temperatures that can used in F8T2 devices where main-chain alignment affects the structure and the performance of devices. The ideal processing condition for maximum alignment of the main chain to the buffing direction comes from heating the sample to 340 °C (above the bulk nematic−isotropic transition temperature of 313 °C) and slowly cooling through the nematic liquid crystal phase to room temperature. This results in an order parameter of $S = 0.88$. However, for prevention of oxidation which may be enhanced by higher temperature processing, similar results can be obtained by heating only to 280 °C and annealing for 5−20 min before cooling to room temperature. The order parameter in this case is still as high as 0.83 as observed by postanneal data which

most closely imitate the annealing conditions of processing. Another important conclusion is that the postanneal and in-situ data are very similar. Both sets of data exhibit the following trends: (a) a relatively high starting value of $S \sim 0.6$, coupled with a positive biaxiality $\eta \sim 0.25$, which is characteristic of a randomly oriented homogeneous thin film; (b) the biaxiality goes to zero for aligned films, indicating the random orientation of fluorene and thiophene units about the molecular axes; (c) in the heating curves, the order parameter reaches a maximum when the films are annealed at 280 °C (above the bulk nematic transition temperatures); (d) heating to 340 °C causes significant ($S \sim 0.7$), but not complete, loss of alignment; and (e) upon cooling, the order parameter increases, reaching a maximum for the heating/cooling cycle upon cooling to room temperature.

Conclusions

Using polarization-dependent near-edge X-ray absorption spectroscopy (NEXAFS), we have looked at the surface structure, particularly the alignment, of thin films of the fluorene−thiophene copolymer F8T2 on buffed and unbuffed polyimide alignment layers. Polarized light microscopy, absorption spectroscopy, and X-ray diffraction show that the use of a rubbed polyimide alignment layer and proper annealing techniques result in large liquid crystal domains in the bulk of the F8T2 films. NEXAFS experiments, which are sensitive to only the top 2 nm of the surface, show that the polymer orientation observed in the bulk of the film is also present at the surface. F8T2 alignment, which originates at the F8T2/polyimide interface, is present throughout the thickness of the thin film. The temperature dependence of surface alignment is studied in detail by taking NEXAFS spectra while samples are heated in a vacuum to a range of temperatures chosen, based on the phase transitions observed by differential scanning calorimetry. These in situ temperature-dependent NEXAFS measurements were also compared to films that were investigated in a postanneal technique, similar to processing. Here, samples were measured at room temperature after various annealing conditions. We found that the in-situ and postanneal data are very similar, meaning that phases observed at elevated temperatures can be frozen in by rapidly cooling the film to room temperature. For both sets of data, order parameter (S) and biaxiality (η) are calculated to give a quantitative description of the alignment of the molecular axis with the rubbing direction (S) and the alignment of the normals to the conjugated segments to the y, z axes (η). η is positive for films that are not aligned, including films deposited on unbuffed polyimide and annealed to temperatures up to 340 °C and films on buffed polyimide that have not been annealed to above the cold crystallization temperature. The positive values $\eta \sim 0.25$ are expected when the F8T2 main-chain axes lie in the $x-y$ plane with random orientation. For aligned films, the orientation of fluorene and thiophene units about the molecular axes remains random, as indicated by values of η decaying to zero ($f_y \approx f_z$). S varies from 0.57 for samples as-deposited by spin-casting without any annealing to 0.88 for samples heated to 340 °C and cooled through the mesophase to room temperature. We see that once heated to the mesophase, the alignment is retained upon further heating or cooling. These results can be used to define processing conditions for F8T2 layers in devices, where it has been shown that the polymer alignment plays a large role in the electronic properties.

Acknowledgment. The authors thank Marvin Paik and Professor Christopher Ober for their interest and input in the project as well as support conducting the NEXAFS experiments. We acknowledge the financial and program support of the Microelectronics Advanced Research Corp. (MARCO) and its Focus Center on Function Engineered NanoArchitectonics (FENA). E.J.K. and A.H. acknowledge support from the National Science Foundation DMR-Polymers Program under Grant DMR03-07233 and from the Office of Naval Research under Grant N00014-02-1-0170. The Materials Research Laboratory of UCSB (funded by the NSF-DMR-MRSEC Program under Grant DMR-0520415) and the National Synchrotron Light Source, Brookhaven National Laboratory, which is supported by the U.S. Department of Energy, Division of Materials Sciences and Division of Chemical Sciences, are also acknowledged for the use of their facilities.

References and Notes

(1) Bao, Z. *Adv. Mater.* **2000**, *12*, 227−230.
(2) Chen, X. L.; Lovinger, A. J.; Bao, Z. N.; Sapjeta, J. *Chem. Mater.* **2001**, *13*, 1341−1348.
(3) Garnier, F.; Horowitz, G.; Fichou, D.; Yassar, A. *Supramol. Sci.* **1997**, *4*, 155−162.
(4) Garnier, F.; Yassar, A.; Hajlaoui, R.; Horowitz, G.; Deloffre, F.; Servet, B.; Ries, S.; Alnot, P. *J. Am. Chem. Soc.* **1993**, *115*, 8716−8721.
(5) Sirringhaus, H.; Brown, P. J.; Friend, R. H.; Nielsen, M. M.; Bechgaard, K.; Langeveld-Voss, B. M. W.; Spiering, A. J. H.; Janssen, R. A. J.; Meijer, E. W. *Synth. Met.* **2000**, *111*, 129−132.
(6) Sirringhaus, H.; Wilson, R. J.; Friend, R. H.; Inbasekaran, M.; Wu, W.; Woo, E. P.; Grell, M.; Bradley, D. D. C. *Appl. Phys. Lett.* **2000**, *77*, 406−408.
(7) Swiggers, M. L.; Xia, G.; Slinker, J. D.; Gorodetsky, A. A.; Malliaras, G. G.; Headrick, R. L.; Weslowski, B. T.; Shashidhar, R. N.; Dulcey, C. S. *Appl. Phys. Lett.* **2001**, *79*, 1300−1302.
(8) Grell, M.; Redecker, M.; Whitehead, K. S.; Bradley, D. D. C.; Inbasekaran, M.; Woo, E. P.; Wu, W. *Liq. Cryst.* **1999**, *26*, 1403−1407.
(9) Lieser, G.; Oda, M.; Miteva, T.; Meisel, A.; Nothofer, H. G.; Scherf, U.; Neher, D. *Macromolecules* **2000**, *33*, 4490−4495.
(10) Kinder, L.; Kanicki, J.; Petroff, P. *Synth. Met.* **2004**, *146*, 181−185.
(11) Pattison, L. R.; Hexemer, A.; Kramer, E. J.; Petroff, P. M.; Fischer, D. A. *Proc. SPIE Int. Soc. Opt. Eng.* **2005**, 5938.
(12) Genzer, J.; Kramer, E. J.; Fischer, D. A. *J. Appl. Phys.* **2002**, *92*, 7070−7079.
(13) Jung, Y.; Cho, T. Y.; Yoon, D. Y.; Frank, C. W.; Lüning, J. *Macromolecules* **2005**, *38*, 867−872.
(14) Geary, J. M.; Goodby, J. W.; Kmetz, A. R.; Patel, J. S. *J. Appl. Phys.* **1987**, *62*, 4100−4108.
(15) Stöhr, J.; Samant, M. G. *J. Electron Spectrosc.* **1999**, *98*−*99*, 189−207.
(16) Stöhr, J.; Samant, M. G.; Lüning, J.; Callegari, A. C.; Chaudhari, P.; Doyle, J. P.; Lacey, J. A.; Lien, S. A.; Purushothaman, S.; Speidell, J. L. *Science* **2001**, *292*, 2299−2302.
(17) Samant, M. G.; Stöhr, J.; Brown, H. R.; Russell, T. P.; Sands, J. M.; Kumar, S. K. *Macromolecules* **1996**, *29*, 8334−8342.
(18) Stöhr, J.; Samant, M. G.; Cossy-Favre, A.; Díaz, J.; Momoi, Y.; Odahara, S.; Nagata, T. *Macromolecules* **1998**, *31*, 1942−1946.
(19) Rosenberg, R. A.; Love, P. J.; Rehn, V. *Phys. Rev. B* **1986**, *33*, 4034.
(20) Kawana, S.; Durrell, M.; Lu, J.; Macdonald, J. E.; Grell, M.; Bradley, D. D. C.; Jukes, P. C.; Jones, R. A. L.; Bennett, S. L. *Polymer* **2002**, *43*, 1907−1913.
(21) Leclère, P.; Hennebicq, E.; Calderone, A.; Brocorens, P.; Grimsdale, A. C.; Müllen, K.; Brédas, J. L.; Lazzaroni, R. *Prog. Polym. Sci.* **2003**, *28*, 55−81.
(22) Stöhr, J.; Outka, D. A. *Phys. Rev. B* **1987**, *36*, 7891−7905.
(23) This definition of S differs from that used by Stöhr and Samant[15] and Jung et al.,[13] who define S of the π^* TDM relative to the surface normal (z-axis). Defining S of the molecular axis as we do here allows comparison of this value with the conventional uniaxial order parameter of a nematic liquid crystal.
(24) Though $\eta > 0$, the positive value of η is not as large as for the case of a perfectly random, homogeneous film, showing that there is some preferential on-edge alignment of the molecules at the surface or some out of plane tilt of molecular axes, but this is very slight. The decay in η with high-temperature annealing could be due to the rotation of molecular axes out of the substrate plane as thermal energy increases, allowing out-of-plane tilt.

MA0521912